C. R. Physique 15 (2014) 441–447

Contents lists available at ScienceDirect

Comptes Rendus Physique

www.sciencedirect.com

Electromagnetism / Électromagnétisme

Goniopolarimetry: Space-borne radio astronomy with imaging capabilities

Goniopolarimétrie : Imagerie en radioastronomie spatiale

Baptiste Cecconi

LESIA, CNRS – Observatoire de Paris – UPMC – Université Denis-Diderot, 5, place Jules-Janssen, 92195 Meudon cedex, France

ARTICLE INFO

Article history:
Available online 13 April 2014

Keywords:
Radioastronomy
Space Physics
Goniopolarimetry
Auroral Physics

Mots-clés :
Radioastronomie
Physique spatiale
Goniopolarimétrie
Physique Aurorale

ABSTRACT

The principles of space-based low-frequency radio astronomy (below 50 MHz) are briefly introduced. As the wavelength range considered does not allow the use of focusing systems, goniopolarimetric (or direction-finding) techniques have been developed. These inversion techniques provide the direction of the wave vector, the polarization state and the flux of the observed electromagnetic wave. In case of spatially extended sources, we can also infer an order of magnitude of the apparent source size. These techniques are presented, and their limitations are discussed. An example from a recent study illustrates the techniques and capabilities.

RÉSUMÉ

La radioastronomie basse fréquence (en dessous de 50 MHz) couvre principalement l'étude des émissions radio planétaires et solaires. Comme la gamme de longueur d'onde considérée ne permet pas l'utilisation de systèmes focalisants, les techniques d'inversion goniopolarimétrique ont été développées. Ces inversions fournissent la direction du vecteur d'onde, l'état de polarisation et la densité spectrale de puissance d'une onde électromagnétique observée. Dans le cas de sources radio spatialement étendues, on peut aussi obtenir l'ordre de grandeur de la taille apparente de la source. Ces techniques sont présentées, ainsi que leurs limitations. Un exemple tiré d'une étude récente illustre ces techniques.

1. Introduction

The frequency band of interest for low-frequency radio astronomy ranges from a few kHz to several tens of MHz (see Fig. 1a for planetary radio emissions). In this frequency range, the corpuscular description is never used, the electromagnetic wave description is used instead. The sampled wave quantities are then the electric and/or magnetic field components. Space-based radio instrumentation and interplanetary missions, such as the *Voyager*, *Galileo* or *Cassini* missions, are required

E-mail address: baptiste.cecconi@obspm.fr.

http://dx.doi.org/10.1016/j.crhy.2014.02.005
1631-0705/

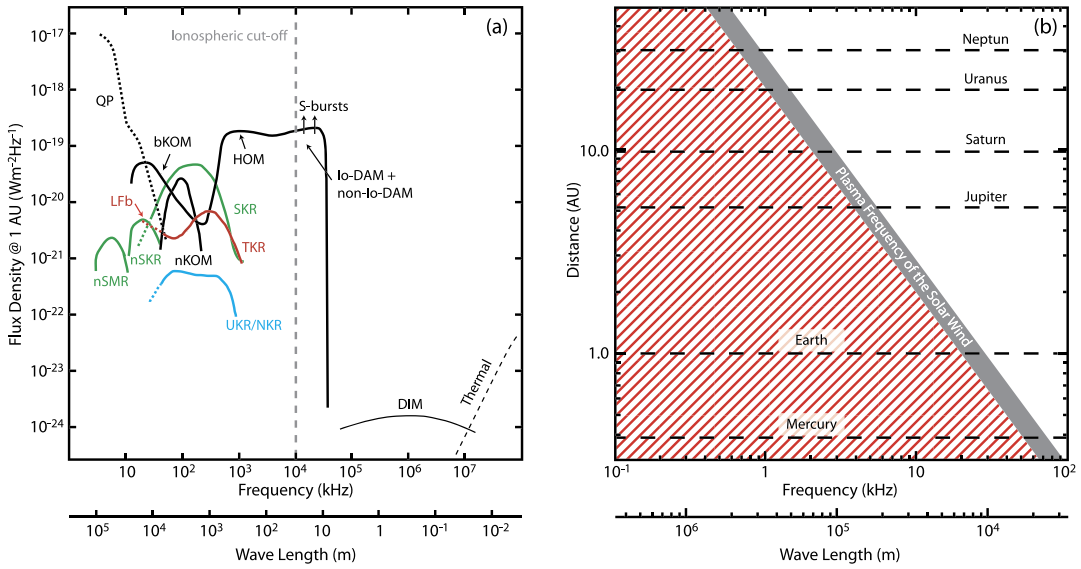

Fig. 1. (a) Typical spectra for planetary radio emissions in the solar system. The flux density is given in W/m^2/Hz, as observed from a distance of 1 AU (Astronomical Unit $= 150 \times 10^9$ m). The radio emissions from Jupiter are in black (nKOM: narrowband Kilometric Radiation; bKOM: broadband Kilometric Radiation; QP: Quasi-Periodic bursts; HOM: Hectometric Radiation; S-bursts: short (or millisecond) bursts; Io-DAM: Io-controlled Decametric Radiation; non-Io-DAM: non-Io-controlled Decametric Radiation; DIM: Decimetric Radiation; Thermal: black body thermal radiation); from Saturn in green (nSMR: narrowband Saturn Myriametric Radiation; nSKR: narrowband Saturn Kilometric Radiation; SKR: Saturn Kilometric Radiation); from the Earth in red (LFb: Low-Frequency bursts; TKR (or AKR): Terrestrial (or Auroral) Kilometric Radiation); and from Uranus and Neptune in blue (UKR/NKR: Uranus/Neptune Kilometric Radiation). The vertical gray dashed line represents the Earth's ionospheric cut-off. Figure adapted from [1], updated with [2–4]. (b) Typical range (gray area) of the plasma frequency in the solar wind with respect to the distance from the Sun. The gray area vertical thickness represents the typical interval of the variation of the plasma frequency in the solar wind. As the plasma frequency is a low-frequency cut-off for free-space propagating electromagnetic waves, radio waves cannot propagate in the red hatched area. Figure adapted from [5]. For interpretation of references to color, see the online version of this article.

due to several constraints: (i) radio emission below 10 MHz cannot be observed from the ground because of the Earth's ionosphere; (ii) low-frequency emission of the outer planets cannot be observed from the vicinity of the Earth, because of the solar wind plasma frequency cutoff (see Fig. 1b); (iii) the space environment of the Earth is polluted by man-made radio interferences above 10 MHz. Given this last point, an option not discussed here relies on lunar-based observations from the far side of the Moon.

The angular resolution of a classical telescope, with a "dish" reflector concentrating radio waves onto an array of antennas that will record the image formed at the focal plane of the telescope, is defined by λ/D, where λ is the wavelength of observation and D the aperture size of the telescope. The size required for such a telescope ($\approx$1 to 10^4 km for $\lambda/D \ll 1$) is totally unrealistic for space-based observations. Hence, simple electric dipoles with a length L of a few meters (or tens of meters) are usually used. They have a poor intrinsic angular resolution ($\lambda/L \approx 1$). Goniopolarimetric (GP) techniques (allowing retrieval of flux, polarization state and direction of arrival of an observed electromagnetic wave) have therefore been developed in order to achieve angular resolution from measurements recorded with these antennas.

In this paper, we will present the antennas and receivers used for space-based radio astronomy, discussing the specific requirements for GP analysis. The different existing goniopolarimetric techniques are presented, as well as their limitations and sources of errors. They are illustrated by a recent study: source location of the Saturn Kilometric Radiation with Cassini data [6]. Another method based on very long baseline interferometry (VLBI) with several spacecraft is also briefly discussed.

2. Instrumentation

Two key elements of a radio instrument are the antenna and the receiver. The antenna is the sensing device: it transforms the electromagnetic fluctuations of the medium surrounding the spacecraft into voltage fluctuations that can be measured by the receiver. The receiver is the measuring device: it converts the voltage at the antenna feeds into a set of parameters (spectral flux density, amplitude, phase…) that are recorded by a data-processing unit (DPU).

The classical space-based instrumentation constraints apply: low mass, low power consumption, small size, reliability, robustness to vibration and radiation. Following recent technological developments, e.g., miniaturization with application of specific integrated circuits (ASICs), it is possible to build versatile low-noise radio receivers with very low mass and low power consumption. However, the main limitation still lies in the electrical sensors. They must be light and their length usually implies that they have to be deployed after launch. Hence, their deployment mechanisms have also to be light and reliable.

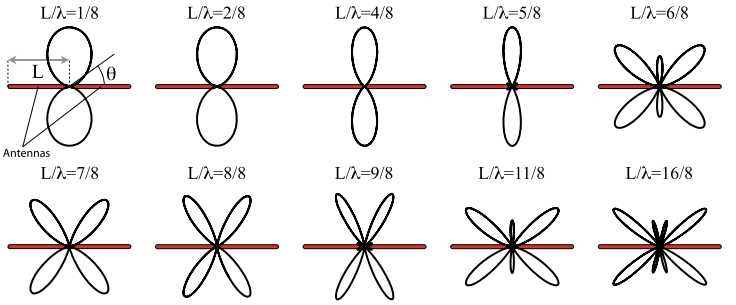

Fig. 2. Beaming pattern of thin boom antennas for various L/λ values. The definition of angle θ is shown on the upper left panel. The antenna pattern is single lobed (with a null in the antenna direction) for short antennas, i.e. up to $L/\lambda \leqslant 1/2$. When $L/\lambda < 1/10$ the antenna pattern does not vary with frequency. With long antennas, it becomes multilobed ($L/\lambda > 1/2$). Figure adapted from [8].

Depending on the primary objectives of the mission, the spacecraft can be either spinning (plasma, particles and fields science objectives) or 3-axis stabilized (imaging science objectives). The radio science objectives together with the spacecraft attitude will drive the characteristics of the antenna (length, orientation, type, etc.) mounted on the spacecraft and those of the associated radio receiver.

We will concentrate in the following paragraph on electric wire antennas. Detailed description for other sensors can be found in [7].

2.1. Electric wire antennas

We thus use electric wire antennas that can be either a monopole or a dipole. In case of a monopole, the instantaneous voltage is probed between the antenna and the spacecraft body, while in the case of a dipole, the differential voltage is probed between the two poles of the antenna. Considering the spacecraft as an infinite conductive plane, the monopole and spacecraft body system would be strictly equivalent to a dipole antenna. In reality, the spacecraft is smaller than the monopole length and is not planar. The beaming pattern of the effective antenna will thus be altered from that of the physical antenna.

The voltage measured at the antenna feeds depends on the instantaneous currents on the antenna, which depend on the antenna's length and shape. In Fig. 2, we show the beaming pattern of a thin boom dipole for various values L/λ. When the antenna is short compared to the wavelength[1] ($L < \lambda/10$), the electric field of the wave is almost constant on the length of the antenna. The voltage measured at the antenna feeds is thus $V = \vec{E}(t).\vec{h}_{\text{eff}} \approx E(t)h_{\text{eff}}\sin\theta$, with θ the angle between the effective antenna vector ($\vec{h}_{\text{eff}}$) and the wave vector $\vec{k}$. The same formalism holds when the antenna length is longer ($L > \lambda/10$), but the effective antenna vector $\vec{h}_{\text{eff}}$ becomes complex and its magnitude depends on the wave vector direction.

2.2. Receivers

A radio receiver, consisting of a series of devices that amplify, filter and sample the signals probed by the antennas, provides spectral power series of data. Some radio receivers can record waveform data, but they will not be described here.

2.2.1. General characteristics

Solar or planetary radio emissions are very bursty and show a wide range of flux densities (see Fig. 1a). Hence, a space-based radio receiver requires low noise and large dynamic range. In currently used radio receivers (e.g., Cassini/RPWS/HFR [9], STEREO/Waves [10]), the amplification of the signal is split into two stages. Preamplifiers are directly connected with the antenna feeds and amplify the signal with a fixed gain before any filtering. Following filtering to the frequency band of analysis, an automatic gain control (AGC) loop adjusts the signal level to adapt it to the sampling analog-to-digital converter (ADC). This design provides $\approx$ 90 dB dynamic range for the Cassini/RPWS/HFR and STEREO/Waves receivers. The instantaneous gain of the AGC loop is recorded, as well as the power measured with the ADC, to allow measurement of the input signal strength. The integration time Δt and frequency bandwidth Δf of the measurements can usually be adjusted. As the relative measurement noise is proportional to $(\Delta t \Delta f)^{-1/2}$, it is not possible to achieve both high temporal and spectral resolution simultaneously.

2.2.2. Multi-channel receivers

The radio receiver may have several input channels. A single-channel receiver can only measure the power received by the connected antenna. The first generations of space-based radio receivers were single-channel receivers such as on the *Hawkeye 1* spacecraft [11]. This type of receiver is also flying on the *JUNO* mission. Dual-channel receivers can use

[1] This wavelength range is called the short antenna or quasistatic range.

the signals provided by two antennas simultaneously. Such receivers provide spectral power series for both antennas and, depending on the receiver's design, cross-correlation series of the signals measured on each antenna. The Cassini/RPWS/HFR and STEREO/Waves receivers include such cross-correlation measurements.

2.2.3. Antenna synthesis

A probe dipole antenna or a perfect wire dipole antenna consists of two identical antenna elements which are aligned in the case of a wire antenna. It is also possible to combine the output of any pair of monopoles. This is called "antenna synthesis". V-shaped wire dipoles are often used, e.g., on Cassini/RPWS/HFR or STEREO/Waves, and consist of two wire monopoles that are not aligned. The antenna synthesis may also involve a phase shift on one of the input signals. Thus the Interball/POLRAD [12,13] radio receiver has nine channels with a set of three orthogonal antennas (x, y and z). Each channel provides a given combination of the antenna signals: the power densities on each of the three antennas (S_x, S_y, S_z) and the power densities of combined signals in phase and in quadrature (S_{x+y}, S_{y+z}, S_{z+x}, $S_{x+\mathrm{i}y}$, $S_{y+\mathrm{i}z}$, $S_{z+\mathrm{i}x}$). Synthetic antennas are usually used to simulate antennas with effective directions that would not have met the required constraints, such as: off-axis and off-spin plane antennas on a spinning spacecraft, or antenna directions that would have interfered with the field of view of an imaging instrument on a 3-axis stabilized spacecraft.

2.3. Calibration

The antenna calibration consists in determining the antenna's beaming pattern. There are three ways of calibrating an antenna response: (i) rheometric analysis, consisting in measuring the electrostatic response of a small model of the spacecraft and its antennas when placed in a tank filled with a dielectric medium [14]; (ii) wire-grid electromagnetic modeling [15]; (iii) inflight measurement of the antenna response with known radio sources [16,17]. When using a wire monopole in the quasistatic range, the calibration simply provides the effective length (including the gain and attenuation due to the base capacitance) and direction of the equivalent electric dipole.

The receiver calibration provides the parameters required to convert the recorded parameters into the wave parameters probed by the antennas. It thus provides the gain of each of its channels for any operating mode. When the receiver provides cross-correlation measurements, the phase shift between the different channels of the receiver has to be calibrated, too.

2.4. Goniopolarimetric measurements

In the quasi-static frequency range, the voltage induced by an incoming electromagnetic wave is $V_{\mathrm{el}} = \vec{h} \cdot \vec{E}$, where $\vec{h}$ is the effective antenna vector and $\vec{E} = \vec{E}_0\, \mathrm{e}^{\mathrm{i}\omega t}$ is the electric field of the wave. A GP radio receiver measures a series of correlation values $P_{ij} = \langle V_i V_j^* \rangle$. A transverse electromagnetic plane wave (i.e., emitted by a point radio source at infinity) is characterized by its Stokes parameters (S the flux, Q, U, the linear polarization degrees, and V the circular polarization degree) and the wave vector $\vec{k}$ direction which is defined by its colatitude θ and azimuth ϕ in a given frame. A model for the voltage correlation P_{ij} expression can be found in [18] or in [17] in case of a point source and in [19] in case of an extended source.

The GP capabilities of a radio receiver depend on the receiver design and especially on the number of independent analysis channels, i.e., the number of simultaneous correlation measurements. For single-channel receivers, only one autocorrelation is measured, whereas for dual-channel receivers that are connected with two antennas, up to two autocorrelations (one on each antenna) and a complex cross-correlation may be measured. In order to increase the capabilities of the radio receivers with one or more analysis channels, successive measurements at the same frequency, but on different pairs of antenna, can be performed quasi-instantaneously.

There are two possible ways to achieve GP on space-borne radio receivers: (i) spin demodulation GP on a spinning spacecraft, like *Geotail*, *Wind* and *Ulysses*; and (ii) instantaneous GP on a 3-axis stabilized spacecraft, like Cassini and STEREO. Each of these GP techniques may provide the direction of arrival of the wave, flux, polarization and angular size of the source. At the time of writing, inversions providing the size of the source exist for spin demodulation GP, while the development of such inversions is in progress in the *STEREO*/Waves team for a 3-axis stabilized spacecraft. These inversions will be based on the model-expression of the measurements in the case of an extended source [19].

2.5. Sources of uncertainty

Several sources of uncertainty may alter or bias the GP measurements and results. Some sources of error such as the signal-to-noise ratio and digitization noise depend on the receiver setup. The electromagnetic environment also induces noise: galactic background emission (resulting from the free–free interactions of the electrons in the Galactic magnetic field), local plasma noise and photoelectron noise, and interference lines from the spacecraft. The source variability, its apparent size and the fact that we can observe several sources at the same time, may also induce errors in the results (see Fig. 3). Complete discussions of these uncertainty sources may be found in [17–19].

As the antennas measure the electric field of electromagnetic waves passing in the vicinity of the spacecraft, GP techniques only measure the local direction of the wave vector. When propagation effects occur between the source and the

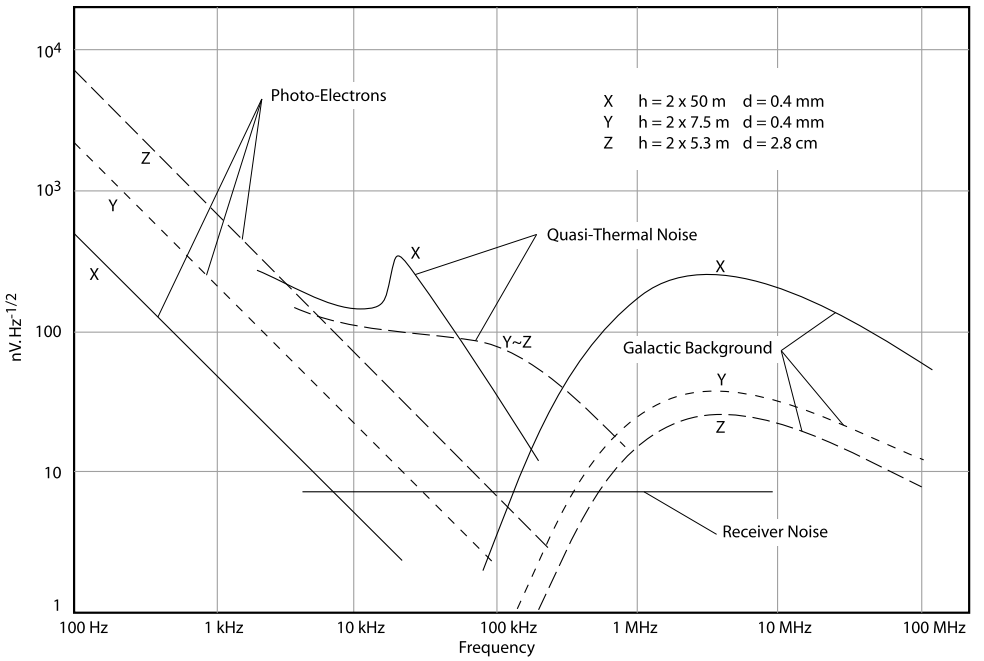

Fig. 3. Noise sources and noise levels for space-based radio receivers. Interference lines due to other instruments or originating from power converters can add to the displayed spectra. The noise spectra are traditionally given as a square root of a spectral power, i.e., in units of 1 $\mathrm{nV\,Hz^{-\frac{1}{2}}}$. The noise levels are provided for various antenna characteristics (h is the antenna length and d its diameter). Type *X* antennas correspond to *Wind* antennas, for instance. Figure adapted from [20].

spacecraft, e.g., refraction and diffusion, modeling of the ray path between the source and the spacecraft is necessary. Particular care is needed when the local plasma frequency along the path of the wave is close to the wave frequency.

Careful data selection is essential in order to obtain accurate GP measurements. In the case of Cassini/RPWS/HFR, the selection criteria for a typical accuracy are given in [17].

3. Example of a GP result: Saturn kilometric radiation source location

Many papers have been published using the GP techniques described in the previous sections. A recent study [6] is highlighted here: the source location of the Saturn kilometric radiation using GP data provided by Cassini/RPWS/HFR.

The Cassini spacecraft has orbited Saturn since July 2004, exploring various orbital distances, latitudes and local times (LT). During the 24 hours of data presented in that study, the radio receiver was operating in two-antenna mode. In order to find the source location, several assumptions were made: (i) the observed radio waves were circularly polarized; (ii) straight propagation between the source and the spacecraft; (iii) an emission process is proposed, which implies that the wave is emitted at the local electron cyclotron frequency f_c. With these assumptions, the source is located where the straight line defined by the direction of arrival intersects the $f = f_c$ iso-surface, which is computed using a planetary magnetic field model. Once the source is located, it is possible to compute the footprint location of the active magnetic field line. Fig. 4 shows an example of GP results and source localization.

The observed radio waves are all left-handed (LH) polarized, and come from the southern hemisphere, which is characteristic of an R–X mode emission. On the left panel of Fig. 4, there are two series of source locations, on each side of the meridian of Cassini. The western part, on the left of the meridian, corresponds to sources that are almost all on the same magnetic field line, whose footprint is at $\approx -68°$ latitude and $\approx$ 07:00 LT, as shown on the right panel. The eastern part, on the right of the meridian of *Cassini*, corresponds to sources at $\approx -70°$ latitude, and between 13:00 and 15:00 LT. The footprint location found in that study is fully consistent with the locus of the ultraviolet aurora.

4. Conclusion

The GP techniques allow radio astronomers to rebuild the wave parameters from space-based radio instruments, despite the poor angular resolution of electric antennas. From the example presented above, it is clear that the GP techniques provide a very powerful tool that can yield the flux density of the observed radio wave, its polarization state, the direction of the wave vector, and possibly the size of the source. Thanks to careful data selection, it is possible to produce radio emission maps (see the left panel of Fig. 4). The main advantage of this imaging technique is that it is possible to build a posteriori any maps with selection on time, frequency, polarization, etc. These imaging capabilities are not possible with

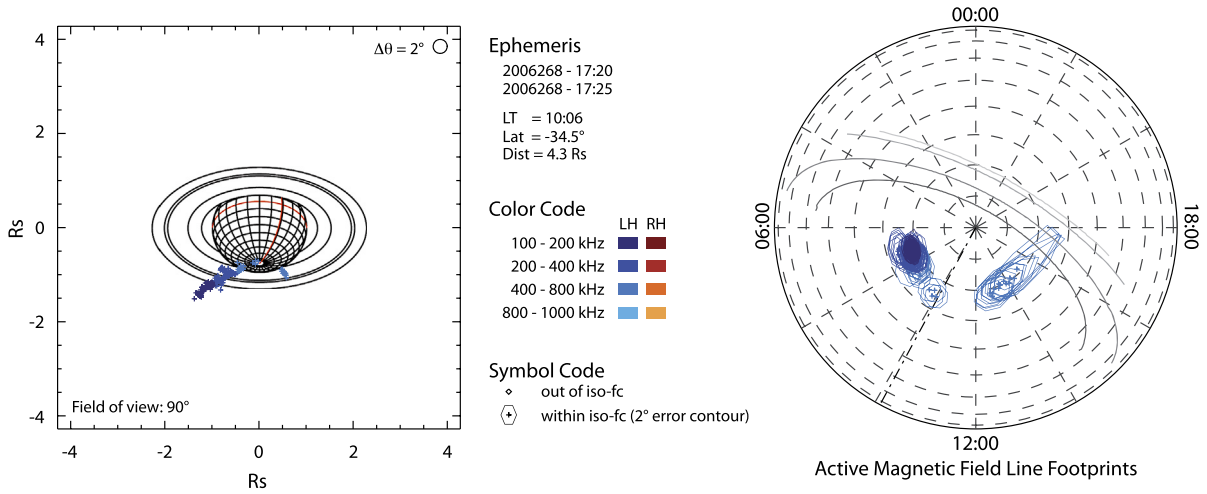

Fig. 4. Saturn Kilometric Radiation (SKR) source localization with Cassini/RPWS/HFR data on day 2006-268, between 17:20 and 17:25, spacecraft event time. The Cassini spacecraft was located at 10:06 LT, in the southern hemisphere (−34.5° southern latitude), and at 4.3 Saturn radii from the center of the planet. Left panel: computed directions of arrival as seen from Cassini. Right panel: footprints of the magnetic field lines supporting the radio sources, on a view of the southern pole of Saturn. Note that magnetic poles are aligned with the rotation axis, at Saturn. The center of the figure is the South Pole and each dashed circle is a 10° latitudinal separation. The local time is displayed around the equatorial circle: "12:00" represents the meridian containing the Sun. On that panel, the mixed lines (dash–dot) represent the meridian containing Cassini, and the gray curves delimit the visible portion of the $f = f_c$ iso-surface, for each of the four frequency ranges. Left-handed radio emissions are observed (blue) from 100 kHz to 800 kHz. No right-handed (red) emission is observed. This figure is adapted from [6]. For interpretation of references to color, see the online version of this article.

classical imaging instruments. The main drawback is that it is usually necessary to make assumptions about the wave (or source) parameters in order to invert GP measurements. However, it is clear from the study of Saturn presented above that GP results can be strongly enhanced when coupled with physical models such as planetary magnetic field and plasma density models along with an understanding of the source emission process.

Acknowledgement

The author acknowledges CNES (Centre national d'études spatiales) for supporting Cassini/RPWS and STEREO/Waves studies.

References

[1] P. Zarka, The auroral radio emissions from planetary magnetospheres: What do we know, What don't we know, what do we learn from them?, Adv. Space Res. 12 (8) (1992) 99–115.
[2] P. Zarka, B. Cecconi, W.S. Kurth, Jupiter's low-frequency radio spectrum from Cassini/Radio and Plasma Wave Science (RPWS) absolute flux density measurements, J. Geophys. Res. 109 (2004) A09S15, http://dx.doi.org/10.1029/2003JA010260.
[3] L. Lamy, P. Zarka, B. Cecconi, R. Prangé, W.S. Kurth, D.A. Gurnett, Saturn kilometric radiation: average and statistical properties, J. Geophys. Res. 113 (2008) A07201, http://dx.doi.org/10.1029/2007JA012900.
[4] L. Lamy, P. Zarka, B. Cecconi, R. Prangé, AKR diurnal, semi-diurnal and shorter term modulations disentangled by Cassini/RPWS observations, J. Geophys. Res. 115 (2014) A09221, http://dx.doi.org/10.1029/2010JA015434.
[5] P. Zarka, Radio emissions from the planets and their moons, in: R.G. Stone, K.W. Weiler, M.L. Goldstein, J.-L. Bougeret (Eds.), Radio Astronomy at Long Wavelengths, in: Geophysical Monograph, vol. 119, AGU, Washington, DC, 2000, pp. 167–178.
[6] B. Cecconi, L. Lamy, P. Zarka, R. Prangé, W.S. Kurth, P. Louarn, Goniopolarimetric study of the Rev 29 perikrone using the Cassini/RPWS/HFR radio receiver, J. Geophys. Res. 114 (2009) A03215, http://dx.doi.org/10.1029/2008JA013830.
[7] B. Cecconi, Goniopolarimetric techniques for low-frequency radio astronomy, in: ISSI/ESA, May 2009, pp. 263–277.
[8] H. Jasik, Antenna Engineering Handbook, McGraw–Hill, New York, Toronto and London, 1961.
[9] D.A. Gurnett, et al., The Cassini radio and plasma wave science investigation, Space Sci. Rev. 114 (2004) 395–463, http://dx.doi.org/10.1007/s11214-004-1434-0.
[10] J.-L. Bougeret, K. Goetz, M.L. Kaiser, S.D. Bale, P.J. Kellogg, M. Maksimovic, N. Monge, S.J. Monson, P.L. Astier, S. Davy, M. Dekkali, J.J. Hinze, R.E. Manning, E. Aguilar-Rodriguez, X. Bonnin, C. Briand, I.H. Cairns, C.A. Cattell, B. Cecconi, J. Eastwood, R.E. Ergun, J. Fainberg, S. Hoang, K.E.J. Huttunen, S. Krucker, A. Lecacheux, R.J. MacDowall, W. Macher, A. Mangeney, C.A. Meetre, X. Moussas, Q.N. Nguyen, T.H. Oswald, M. Pulupa, M.J. Reiner, P.A. Robinson, H. Rucker, C. Salem, O. Santolik, J.M. Silvis, R. Ullrich, P. Zarka, I. Zouganelis, S/Waves: The radio and plasma wave Investigation on the STEREO Mission, Space Sci. Rev. 136 (2008) 487–528, http://dx.doi.org/10.1007/s11214-007-9298-8.
[11] W.S. Kurth, M.M. Baumback, D.A. Gurnett, Direction-finding measurements of auroral kilometric radiation, J. Geophys. Res. 80 (1975) 2764–2770.
[12] J. Hanasz, Z. Krawczyk, M.M. Mogilevsky, R. Schreiber, H. de Feraudy, K. Dudzinski, T.V. Romantsova, W. Nowakiewicz, A. Kraynyuk, M. Barylko, A. Buczkowska, J. Juchniewicz, V.N. Nazarov, N. Mikhalev, Observation of Auroral Kilometric Radiation on the INTEBALL-2 satellite: The POLRAD experiment, Cosm. Res. 36 (1998) 575.
[13] J. Hanasz, R. Schreiber, H. de Feraudy, M.M. Mogilevsky, T.V. Romantsova, Observations of the upper frequency cutoffs of the auroral kilometric radiation, Ann. Geophys. 16 (1998) 1097–1104.
[14] H.O. Rucker, W. Macher, R. Manning, H.P. Ladreiter, Cassini model rheometry, Radio Sci. 31 (1996) 1299–1312, http://dx.doi.org/10.1029/96RS01972.

[15] T.H. Oswald, W. Macher, H.O. Rucker, G. Fischer, U. Taubenschuss, J.-L. Bougeret, A. Lecacheux, M.L. Kaiser, K. Goetz, Various methods of calibration of the STEREO/Waves antennas, Adv. Space Res. 43 (3) (2009) 355–364, http://dx.doi.org/10.1016/j.asr.2008.07.017.
[16] D.F. Vogl, et al., In-flight calibration of the Cassini-Radio and Plasma Wave Science (RPWS) antenna system for direction-finding and polarization measurements, J. Geophys. Res. 109 (2004) A09S17, http://dx.doi.org/10.1029/2003JA010261.
[17] B. Cecconi, P. Zarka, Direction finding and antenna calibration through analytical inversion of radio measurements performed using a system of 2 or 3 electric dipole antennas, Radio Sci. 40 (2005) RS3003, http://dx.doi.org/10.1029/2004RS003070.
[18] A. Lecacheux, Direction finding of a radiosource of unknown polarization with short electric antennas on a spacecraft, Astron. Astrophys. 70 (1978) 701–706.
[19] B. Cecconi, Influence of an extended source on goniopolarimetry (or direction finding) with Cassini and STEREO radio receivers, Radio Sci. 42 (2007) RS2003, http://dx.doi.org/10.1029/2006RS003458.
[20] R. Manning, Instrumentation for space-based low frequency radio astronomy, in: R.G. Stone, K.W. Weiler, M.L. Goldstein, J.-L. Bougeret (Eds.), Radio Astronomy at Long Wavelengths, in: Geophysical Monograph, vol. 119, AGU, Washington, DC, 2000, pp. 329–337.